Journal of Enzyme Inhibition and Medicinal Chemistry

ISSN: 1475-6366 (Print) 1475-6374 (Online) Journal homepage: http://www.tandfonline.com/loi/ienz20

Discovery of novel dual inhibitors of receptor tyrosine kinases EGFR and IGF-1R

Cornelius Hempel, Frank Totzke, Christoph Schächtele, Abdulkarim Najjar, Wolfgang Sippl, Christoph Ritter & Andreas Hilgeroth

To cite this article: Cornelius Hempel, Frank Totzke, Christoph Schächtele, Abdulkarim Najjar, Wolfgang Sippl, Christoph Ritter & Andreas Hilgeroth (2017) Discovery of novel dual inhibitors of receptor tyrosine kinases EGFR and IGF-1R, Journal of Enzyme Inhibition and Medicinal Chemistry, 32:1, 271-276, DOI: 10.1080/14756366.2016.1247062

To link to this article: https://doi.org/10.1080/14756366.2016.1247062

JOURNAL OF ENZYME INHIBITION AND MEDICINAL CHEMISTRY, 2017
VOL. 32, NO. 1, 271–276
http://dx.doi.org/10.1080/14756366.2016.1247062

Taylor & Francis
Taylor & Francis Group

SHORT COMMUNICATION

OPEN ACCESS

Discovery of novel dual inhibitors of receptor tyrosine kinases EGFR and IGF-1R

Cornelius Hempel[a], Frank Totzke[b], Christoph Schächtele[b], Abdulkarim Najjar[a], Wolfgang Sippl[a], Christoph Ritter[c] and Andreas Hilgeroth[a]

[a]Department of Pharmaceutical Chemistry, Institute of Pharmacy, Martin Luther University, Halle, Germany; [b]ProQinase GmbH, Freiburg, Germany; [c]Department of Clinical Pharmacy, Institute of Pharmacy, Ernst Moritz Arndt University Greifswald, Germany

ABSTRACT

Novel 4-benzylamino benzo-anellated pyrrolo[2,3-*b*]pyridines have been synthesized with varied substitution patterns both at the molecular scaffold of the benzo-anellated ring and at the 4-benzylamino residue. With a structural similarity to substituted thieno[2,3-*d*]pyrimidines as epidermal growth factor receptor (EGFR) inhibitors, we characterized the inhibition of EGFR for our novel compounds. As receptor heterodimerization gained certain interest as mechanism of cancer cells to become resistant against novel protein kinase inhibitors, we additionally measured the inhibition of insulin-like growth factor receptor IGF-1R which is a prominent receptor for such heterodimerizations with EGFR. Structure–activity relationships are discussed for both kinase inhibitions depending on the varied substitution patterns. We discovered novel dual inhibitors of both receptor tyrosine kinases with interest for further studies to reduce inhibitor resistance developments in cancer treatment.

ARTICLE HISTORY
Received 10 August 2016
Revised 26 August 2016
Accepted 31 August 2016

KEYWORDS
Benzo-anellated compounds; biological activity; protein kinase inhibitory activity

Introduction

Protein kinase inhibitors have been established as effective tool to combat cancer in case of a deregulation of such protein kinases that are being either overexpressed or overactivated in cancer cells to cause cell proliferation[1]. Early protein kinase inhibitor developments concentrated on single kinases to avoid expected side effects during anticancer therapies with such inhibitors[2]. However, resistance developments against such novel inhibitors occurred due to amino acid substitutions in the inhibitor-binding region of the respective kinase[1,2]. Monoclonal antibodies have been therapeutic alternatives that bind to the extracellular domain of the protein kinase receptor[3,4]. Resistance developments against those antibodies have also been described, and the costs of such therapies are high so that small molecule inhibitors, which act at the intracellular receptor site are attractive target compounds for anticancer drug developments, also to address receptor mutants[5,6,7].

The epidermal growth factor receptor (EGFR) tyrosine kinase is one major target structure in cancer therapies. EGFR is found overexpressed in many epidermal tumors[8,9,10]. With additional contributions to angiogenesis and invasive tumor growth, EGFR contributes to cell proliferation and the formation of metastases[11,12]. Developed EGFR inhibitors have a 4-amino quinazoline molecular scaffold **A** that binds to the protein kinase target structure *via* the N-1 of the pyrimidine partial structure (Figure 1) as shown for erlotinib in Figure 2[13].

In recent studies, the phenyl ring of the quinazoline has been replaced by a thiophene ring leading to novel thienopyrimidines **B** with a 4-benzylamino substitution and various substituted phenyl residues attached to the anellated thiophene ring[14]. Those thienopyrimidines reached activities to inhibit EGFR partially similar to the reported quinazolines.

We developed novel pyrrolopyridines **C** with a 4-benzylamino residues and a benzo-anellation to the pyrrole residue. The compounds have a structural similarity to the substituted thienopyrimidines, and we investigated their potential to inhibit EGFR. We additionally proved their ability to inhibit the insulin-like growth factor receptor (IGF-1R) that contributes to an EGFR resistance mechanism *via* a receptor heterodimerization as will be discussed later. So we discovered novel dual inhibitors of cancer-relevant tyrosine kinases EGFR und IGF-1R.

Experimental

General

Commercial reagents were used without further purification. The bromo-substituted benzylamines have been synthesized *via* *N*-benzylamine phthalimides that underwent a following reaction with hydrazine to release the corresponding amines following literature[15]. The ^{1}H-NMR spectra (400 MHz) were measured using tetramethylsilane as internal standard. Thin-layer chromatography (TLC) was performed on E. Merck 5554 silica gel plates. The electrospray ionization (ESI) spectra were recorded on a Finnigan LCQ Classic mass spectrometer. Infrared (IR) spectra were recorded on a Fourier transform infrared (FT-IR) spectrometer. Elemental analysis indicated by the symbols of the elements was within ±0.4% of the theoretical values and was performed using a Leco CHNS-932 apparatus.

Formation of the 1-(pyridine-2-yl)-1H-benzo[d](1,2,3]triazole 1[16]

About 50 g (420 mmol) 1*H*-benzotriazole was suspended in 220 mL of toluene and then 79.6 g (504 mmol) of 2-bromopyridine

CONTACT Andreas Hilgeroth andreas.hilgeroth@pharmazie.uni-halle.de Department of Pharmaceutical Chemistry, Institute of Pharmacy, Martin Luther University, Wolfgang-Langenbeck-Strasse 4, Halle, 06120, Germany

were added. The mixture was heated under reflux for 23 h and then poured into 1 L of ethylacetate. The precipitate was solved under addition of 100 mL of a potassium hydroxide solution (10%). The resulting phases were separated and the organic layer was washed with 300 mL of the potassium hydroxide solution for two times, dried over sodium sulfate and filtered. After evaporation of the solvent, the resulting product was used without further purification. Yield 80 g (97%); yellow-white needles; mp 110–112 °C; ^{1}H NMR ($CDCl_3$) δ 7.33 (ddd, $J = 7.5$ Hz, 4.9 Hz, 1.0 Hz, 1H, 5′-H), 7.46 (ddd, $J = 8.2$ Hz, 7.0 Hz, 1.1 Hz, 1H, 5-H), 7.61 (ddd, $J = 8.3$ Hz, 7.0 Hz, 1.1 Hz, 1H, 6-H), 7.95 (ddd, $J = 8.3$ Hz, 7.5 Hz, 1.9 Hz, 1H, 4′-H), 8.13 (dt, $J = 8.2$ Hz, 1.1 Hz, 1H, 4-H), 8.31 (dt, $J = 8.3$ Hz, 1H, 3′-H), 8.62 (ddd, $J = 4.9$ Hz, 1.9 Hz, 1H, 6′-H), 8.67 (dt, $J = 8.3$ Hz, 1.1 Hz, 1H, 7-H); MS (ESI), $m/z = 197$ [M + H$^+$].

Formation of the 9-H-pyrido[2,3-b]indole 2[17]

Polyphosphoric acid (29.4 g) was heated in a round flask to 170 °C. Then, 11.4 g (58 mmol) of compound **1** were added under stirring for 3 h at the maintained temperature. Then, 50 mL of water was added and the solution was alkalized with a 10 M potassium hydroxide solution to a pH of 10. After stirring overnight, the suspension was poured into 250 mL of water, cooled down to 0 °C in an ice bath and filtered. Precipitated disodium hydrogen phosphate was washed out with portions of water and the remaining residue was kept under vacuum. Yield 3.6 g (36%); beige solid; mp 201–212 °C; ^{1}H NMR (DMSO-d_6) δ 7.18 (dd, $J = 7.18$ Hz, 4.8 Hz, 1H, 3-H), 7.20 (ddd, $J = 8.0$ Hz, 7.0 Hz, 1.3 Hz, 1H, 6-H), 7.43 (ddd, $J = 8.0$ Hz, 7.0 Hz, 1.2 Hz, 1H, 7-H), 7.48 (ddd, $J = 8.2$ Hz, 1.3 Hz, 0.6 Hz, 1H, 8-H), 8.14 (ddt, $J = 8.0$ Hz, 1.2 Hz, 0.6 Hz, 1H, 5-H), 8.39 (dd, $J = 4.8$ Hz, 1.6 Hz, 1H, 2-H), 8.48 (ddd, $J = 7.7$ Hz, 1.6 Hz, 0.6 Hz, 1H, 4-H), 11.74 (*s*, 1H, 9H); MS (ESI), $m/z = 169$ [M + H$^+$].

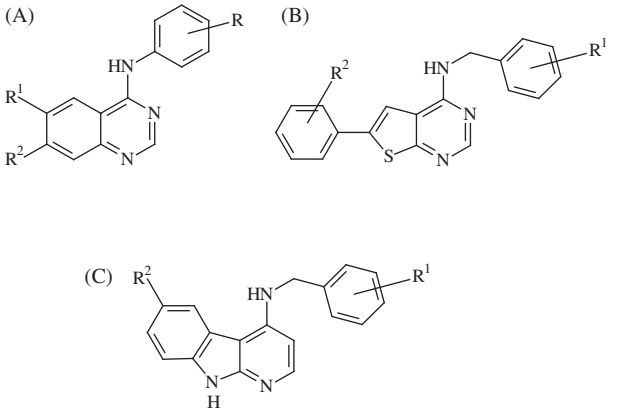

Figure 1. Structure of quinazolines A, thienopyrimidines B and benzopyrrolopyridines C as EGFR inhibitors.

Formation of the 4-chloro-9-H-pyrido[2,3-b]indole 3

About 3.6 g (21 mmol) of compound **2** were dissolved in acetic acid and 4.4 g (45 mmol) of a 35% solution of hydrogen peroxide in water were added dropwise. The solution was heated under reflux for 5 h. Then, the solution volume was reduced in vacuum and the remaining oily product was treated with a saturated potassium carbonate solution to reach a pH of 8. After stirring overnight, the resulting precipitate was filtered off and dried in vacuum. After that 3.6 g (19.5 mmol) were dissolved in dimethylformamide (DMF) under stirring and argon atmosphere. The solution was cooled down to 0 °C on an ice bath, and then, 4.2 mL (7.1 g, 46.9 mmol) of phosphoryl oxychloride was added. The whole mixture was stirred for 24 h and poured into 50 mL of water. The pH value was adjusted to 12 using a 12% solution of potassium hydroxide. After stirring for 30 min, the solution was filtered and the remaining solid was dried and purified by column chromatography using silica gel and a mixture of cyclohexane and ethylacetate (80/20) to wash out the impurities, and then, with the eluent mixture of 50/50 to isolate the poduct **3**. Yield 2.3 g (58%); yellow-white crystals; mp 230–232 °C; ^{1}H NMR (DMSO-d_6) δ 7.32–7.27 (*m*, 1H, 6-H), 7.30 (d, $J = 5.3$ Hz, 1H, 3-H), 7.57–7.50 (*m*, 2H, 7-, 8-H), 8.33 (dd, $J = 8.0$ Hz, 1.3 Hz, 1H, 5-H), 8.36 (d, $J = 5.3$ Hz, 1H, 2-H), 12.16 (*s*, 1H, 9H); MS (ESI), $m/z = 203$ [M + H$^+$]; IR (ATR): 3436, 3262, 3090, 1624, 1597, 1573, 1456, 788, 736 cm^{-1}.

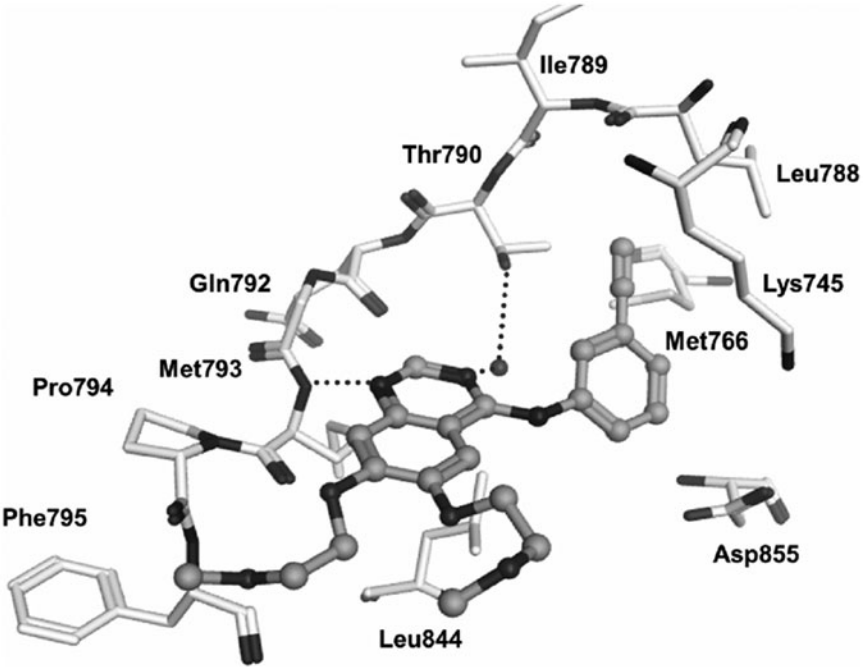

Figure 2. Quinazoline compound erlotinib binding to the hinge region of EGFR with hydrogen bonds.

Formation of the 6-bromo-4-chloro-9-H-pyrido[2,3-b]indole 4

About 1 g (4.9 mmol) of compound **3** was dissolved in 30 mL of acetic acid, and 0.94 g (5.9 mmol) of bromine was added dropwise under stirring. The resulting sticky mixture was diluted with 20 mL of acetic acid and stirring continued for 24 h at room temperature. Then, 50 mL of a 1 M sodium thiosulfate solution was added. The solution was cooled on an ice bath and the pH value was adjusted to 10 with concentrated ammonia. Then extraction followed for three times with each 50 mL chloroform first and then with each 50 mL of ethylacetate. The unified organic layers were dried over sodium sulfate. Then, it was filtered and the layer was removed in vacuum. Yield 1.3 g (94%); yellow-white needles; mp 264–266 °C; ^{1}H NMR (DMSO-d_6) δ 7.36 (d, $J = 5.2$ Hz, 1H, 3-H), 7.53 (d, $J = 8.7$ Hz, 1H, 8-H), 7.67 (dd, $J = 8.7$ Hz, 2.1 Hz, 1H, 7-H), 8.41 (d, $J = 5.2$ Hz, 1H, 2-H), 8.42 (d, $J = 2.1$ Hz, 1H, 5-H), 12.37 (*s*, 1H, 9H); MS (ESI), $m/z = 283$ [M + H$^+$]; IR (ATR): 3436, 3224, 3137, 3074, 1619, 1585, 1566, 1456, 750, 643 cm^{-1}.

General procedure for the formation of the 4-benzylamino substituted 6-bromo-9-H-pyrido[2,3-b]indoles 5a–h

One equivalent of compound **4** and 15 equivalents of the respective benzylamine were heated under stirring at 140 °C for 48 h. After cooling 10 mL of chloroform were added and the mixture was stirred over night. The resulting precipitate was washed with tetrahydrofurane and filtered (Scheme 1).

N^4–(3-Methoxybenzyl)-6-bromo-9H-pyrido[2,3-b]indole-4-amine ***5a***. Yield 0.501 g (73%); white solid; mp 245–248 °C; ^{1}H NMR (DMSO-d_6) δ 3.69 (*s*, 3H, CH_3), 4.59 (d, $J = 6.1$ Hz, 2H, CH_2), 6.24 (d, $J = 5.8$ Hz, 1H, 3-H), 6.78 (d, $J = 8.5$ Hz, 1H, 6′-H), 6.93–7.04 (*m*, 2H, 2′-, 4′-H), 7.22 (*t*, $J = 8.0$ Hz, 1H, 5′-H), 7.25 (*t*, $J = 6.1$ Hz, 1H, CH_2-*N***H**), 7.35 (d, $J = 8.5$ Hz, 1H, 8-H), 7.45 (dd, $J = 8.5$ Hz, 1.8 Hz, 1H, 7-H), 7.92 (d, $J = 5.8$ Hz, 1H, 2-H), 8.65 (d, $J = 1.8$ Hz, 1H, 5-H), 11.61 (*s*, 1H, 9-H); MS (ESI), $m/z = 382$ [M + H$^+$]; IR (ATR): 3457, 3004, 2918, 2834, 1593, 1513, 1489, 1462, 1252, 1033, 873, 786, 777 cm^{-1}. Anal. ($C_{19}H_{16}BrN_3O$) Calc. C 59.7, H 4.2, N 11.0; Found C 59.5, H 4.2, N 10.6.

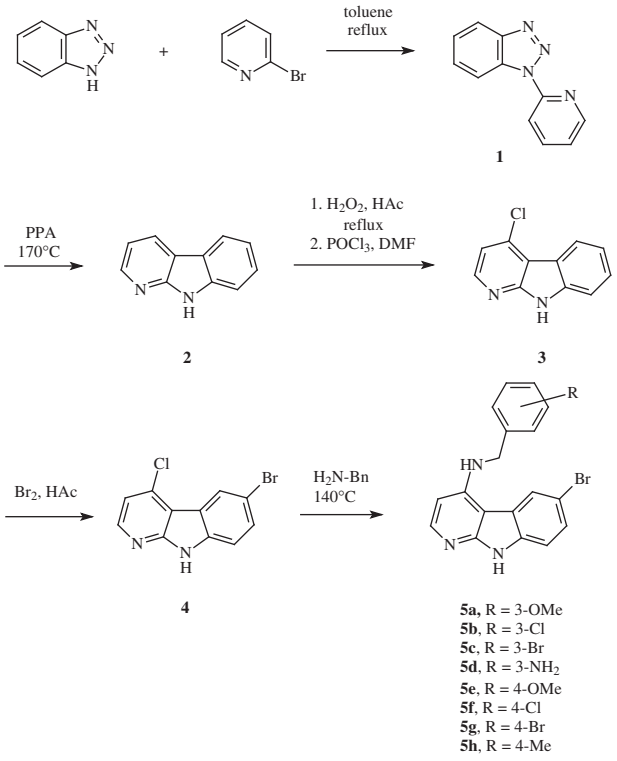

Scheme 1. Formation of 6-bromo-substituted compounds

N^4–(3-Chlorobenzyl)-6-bromo-9H-pyrido[2,3-b]indole-4-amine ***5b***. Yield 0.056 g (14%); yellow crystals; mp 251–253 °C; ^{1}H NMR (DMSO-d_6) δ 4.62 (d, $J = 6.2$ Hz, 2H, CH_2), 6.24 (d, $J = 5.8$ Hz, 1H, 3-H), 7.23–7.49 (*m*, 7H, CH_2-*N***H**), 7-, 8-H, benzylic H), 7.93 (d, $J = 5.8$ Hz, 1H, 2-H), 8.64 (d, $J = 1.8$ Hz, 1H, 5-H), 11.63 (*s*, 1H, 9-H); MS (ESI), $m/z = 388$ [M + H$^+$]; IR (ATR): 3456, 3100, 2915, 2833, 1592, 1572, 1511, 1465, 1433, 1135, 874, 786, 767 cm^{-1}. Anal. ($C_{18}H_{13}BrClN_3$) Calc. C 55.9, H 3.4, N 10.9; Found C 56.2, H 3.8, N 11.00.

N^4–(3-Bromobenzyl)-6-bromo-9H-pyrido[2,3-b]indole-4-amine ***5c***. Yield 0.158 g (37%); white solid; mp 239–241 °C; ^{1}H NMR (DMSO-d_6) δ 4.62 (d, $J = 6.2$ Hz, 2H, CH_2), 6.24 (d, $J = 5.8$ Hz, 1H, 3-H), 7.23–7.31 (*m*, 2H, 5′-H, CH_2-*N***H**), 7.41 (d, $J = 7.9$ Hz, 2H, 4′-, 5-H), 7.54 (d, $J = 8.4$ Hz, 1H, 8-H), 7.60 (*s*, 1H, 2′-H), 7.67 (dd, $J = 8.7$ Hz, 2.0 Hz, 1H, 7-H), 7.94 (d, $J = 5.8$ Hz, 1H, 2-H), 8.64 (d, $J = 2.0$ Hz, 1H, 5-H), 11.65 (*s*, 1H, 9-H); MS (ESI), $m/z = 432$ [M + H$^+$]; IR (ATR): 3448, 3121, 2950, 2830, 1593, 1568, 1512, 1491, 1465, 1445, 1430, 869, 786, 772 cm^{-1}. Anal. ($C_{18}H_{13}Br_2N_3$) Calc. C 50.2, H 3.0, N 9.8; Found C 50.5, H 2.9, N 10.1.

N^4–(3-Aminobenzyl)-6-bromo-9H-pyrido[2,3-b]indole-4-amine ***5d***. Yield 0.069 g (11%); white solid; mp 246–252 °C; ^{1}H NMR (DMSO-d_6) δ 4.47 (d, $J = 6.0$ Hz, 2H, CH_2), 5.12 (br *s*, 2H, NH_2), 6.22 (d, $J = 5.9$ Hz, 1H, 3-H), 6.39 (d, $J = 8.0$ Hz, 1H, 4′-H), 6.53 (d, $J = 7.5$ Hz, 1H, 6′-H), 6.56 (*s*, 1H, 2′-H), 6.94 (dd, $J = 8.0$ Hz, 7.5 Hz, 1H, 5′-H), 7.24 (*t*, $J = 6.0$ Hz, 1H, CH_2-*N***H**), 7.35 (d, $J = 8.6$ Hz, 1H, 8-H), 7.44 (dd, $J = 8.6$ Hz, 1.9 Hz, 1H, 7-H), 7.91 (d, $J = 5.9$ Hz, 1H, 2-H), 8.66 (d, $J = 1.9$ Hz, 1H, 5-H), 11.62 (*s*, 1H, 9-H); MS (ESI), $m/z = 367$ [M + H$^+$]; IR (ATR): 3453, 3371, 3028, 2922, 2836, 1595, 1512, 1489, 1457, 1440, 874, 786, 767 cm^{-1}. Anal. ($C_{18}H_{15}BrN_4$) Calc. C 59.1, H 4.1, N 15.3; Found C 58.8, H 4.2, N 15.1

N^4–(4-Methoxybenzyl)-6-bromo-9H-pyrido[2,3-b]indole-4-amine ***5e***. Yield 0.267 g (38%); white solid; mp 245–249 °C; ^{1}H NMR (DMSO-d_6) δ 3.69 (*s*, 3H, CH_3), 5.54 (d, $J = 6.1$ Hz, 2H, CH_2), 6.25 (d, $J = 5.8$ Hz, 1H, 3-H), 6.86 (d, $J = 8.6$ Hz, 2H, 2′-, 6′-H), 7.22 (*t*, $J = 6.1$ Hz, 1H, CH_2-*N***H**), 7.32 (d, $J = 8.6$ Hz, 2H, 3′-, 5′-H), 7.34 (d, $J = 8.5$ Hz, 1H, 8-H), 7.43 (dd, $J = 8.5$ Hz, 1.8 Hz, 1H, 7-H), 7.91 (d, $J = 5.8$ Hz, 1H, 2-H), 8.64 (d, $J = 1.8$ Hz, 1H, 5-H), 11.58 (*s*, 1H, 9-H); MS (ESI), $m/z = 382$ [M + H$^+$]; IR (ATR): 3428, 3086, 2998, 2932, 1594, 1562, 1510, 1461, 1451, 1281, 1025, 879, 801, 791 cm^{-1}. Anal. ($C_{19}H_{16}BrN_3O$) Calc. C 59.7, H 4.2, N 11.0; Found C 59.5, H 4.2, N 10.6.

N^4–(4-Chlorobenzyl)-6-bromo-9H-pyrido[2,3-b]indole-4-amine ***5f***. Yield 0.236 g (67%); yellow white crystals; mp 263–265 °C; ^{1}H NMR (DMSO-d_6) δ 4.61 (d, $J = 6.2$ Hz, 2H, CH_2), 6.22 (d, $J = 5.8$ Hz, 1H, 3-H), 7.27 (*t*, $J = 6.2$ Hz, 1H, CH_2-*N***H**), 7.35 (d, $J = 8.5$ Hz, 1H, 8-H), 7.36 (d, $J = 8.1$ Hz, 2H, 2′-, 6′-H), 7.42 (d, $J = 8.1$ Hz, 2H, 3′-, 5′-H), 7.45 (dd, $J = 8.5$ Hz, 1.8 Hz, 1H, 7-H), 7.92 (d, $J = 5.8$ Hz, 1H, 2-H), 8.64 (d, $J = 1.8$ Hz, 1H, 5-H), 11.62 (*s*, 1H, 9-H); MS (ESI), $m/z = 388$ [M + H$^+$]; IR (ATR): 3444, 3095, 2918, 2833, 1595, 1576, 1512, 1488, 1465, 1445, 1089, 874, 786, 767 cm^{-1}. Anal. ($C_{18}H_{13}BrClN_3$) Calc. C 55.9, H 3.4, N 10.9; Found C 55.2, H 3.8, N 11.0.

N^4–(4-Bromobenzyl)-6-bromo-9H-pyrido[2,3-b]indole-4-amine ***5 g***. Yield 0.100 g (38%); brownish solid; mp 286–288 °C; ^{1}H NMR (DMSO-d_6) δ 4.60 (d, $J = 6.0$ Hz, 2H, CH_2), 6.22 (d, $J = 5.8$ Hz, 1H, 3-H), 7.30 (*t*, $J = 6.0$ Hz, 1H, CH_2-*N***H**), 7.34–7.40 (*m*, 3H, 2′-, 6′-, 8-H), 7.46 (dd, $J = 8.6$ Hz, 1.7 Hz, 1H, 7-H), 7.51 (d, $J = 8.4$ Hz, 2H, 3′-, 5′-H), 7.93 (d, $J = 5.8$ Hz, 1H, 2-H), 8.65 (d, $J = 1.7$ Hz, 1H, 5-H), 11.64 (*s*, 1H, 9-H); MS (ESI), $m/z = 432$ [M + H$^+$]; IR (ATR): 3459, 3027, 2918, 2835, 1595, 1574, 1513, 1485, 1466, 1448, 874, 786, 767 cm^{-1}. Anal. ($C_{18}H_{13}Br_2N_3$) Calc. C 50.2, H 3.0, N 9.8; Found C 50.2, H 3.1, N 9.7.

N^4–(4-Methylbenzyl)-6-bromo-9H-pyrido[2,3-b]indole-4-amine ***5h***. Yield 0.155 g (24%); yellow crystals; mp 280–284 °C; ^{1}H NMR (DMSO-d_6) δ 2.24 (*s*, 3H, CH_3), 4.56 (d, $J = 6.1$ Hz, 2H, CH_2), 6.22 (d, $J = 5.8$ Hz, 1H, 3-H), 7.10 (d, $J = 8.3$ Hz, 2H, 3′-, 5′-H), 7.17–7.27 (*m*, 1H, CH_2-***N*H**), 7.28 (d, $J = 8.3$ Hz, 2H, 2′, 6′-H), 7.34 (d, $J = 8.5$ Hz, 1H, 8-H), 7.44 (dd, $J = 8.5$ Hz, 1.9 Hz, 1H, 7-H), 7.90 (d, $J = 5.8$ Hz, 1H, 2-H), 8.64 (d, $J = 1.9$ Hz, 1H, 5-H), 11.60 (*s*, 1H, 9-H); MS (ESI), *m/z* = 368 [M + H$^+$]; IR (ATR): 3462, 3098, 3023, 2916, 1595, 1512, 1465, 1445, 1422, 875, 786, 767 cm^{-1}. Anal. ($C_{19}H_{16}BrN_3$) Calc. C 62.3, H 4.4, N 11.5; Found C 61.9, H 4.8, N 11.8.

General procedure for the formation of the 6-cyano substituted 9-H-pyrido[2,3-b]indoles 6a–c

One equivalent of the respective 6-bromo 4-benzylamine compound **5** was dissolved in 3 mL NMP and 2.7 equivalents of copper(I) cyanid were added. Then, the mixture was heated under argon atmosphere and reflux for 7 h at 200 °C and after that poured into 20 mL of ethylacetate. Washing with 10 mL of a 20% solution of ammonia in water followed and a saturated solution of sodium chloride in water was added to clear the suspension formation. The extraction of the water phase with 20 mL ethylacetate followed and the unified organic layers were dried over sodium sulfate, filtered and, finally, the solution volume was reduced in vacuum. Then, 20 mL of water was added so that the product **6** precipitated (Scheme 2).

4–(3-Methoxybenzyl)amino-9H-pyrido[2,3-b]indole-6-carbonitrile ***6a***. Yield 0.331 g (86%); brownish solid; mp 302–304 °C; ^{1}H NMR (DMSO-d_6) δ 3.69 (s, 3H, CH_3), 4.60 (d, $J = 6.2$ Hz, 2H, CH_2), 6.33 (d, $J = 5.8$ Hz, 1H, 3-H), 6.78 (ddd, $J = 8.2$ Hz, 2.6 Hz, 1.0 Hz, 1H, 6′-H), 6.94–7.01 (m, 2H, 2′-, 4′-H), 7.22 (t, $J = 8.2$ Hz, 1H, 5′-H), 7.37 (t, $J = 6.2$ Hz, 1H, CH_2-***N*H**), 7.53 (d, $J = 8.4$ Hz, 1H, 8-H), 7.70 (dd, $J = 8.4$ Hz, 1.5 Hz, 1H, 7-H), 7.98 (d, $J = 5.8$ Hz, 1H, 2-H), 8.96 (s, 1H, 5-H), 12.03 (s, 1H, 9-H); MS (ESI), *m/z* = 329 [M + H$^+$]; IR (ATR): 3414, 2999, 2931, 2834, 2219, 1593, 1573, 1517, 1463, 1259, 1039, 786, 767 cm^{-1}. Anal. ($C_{20}H_{16}N_4$) Calc. C 73.2, H 4.9, N 17.1; Found C 73.1, H 5.1, N 16.7.

4–(4-Methoxybenzyl)amino-9H-pyrido[2,3-b]indole-6-carbonitrile ***6b***. Yield 0.070 g (82%); brownish solid; mp 311–313 °C; ^{1}H NMR (DMSO-d_6) δ 3.69 (s, 3H, CH_3), 4.56 (d, $J = 6.1$ Hz, 2H, CH_2), 6.35 (d, $J = 5.8$ Hz, 1H, 3-H), 6.87 (d, $J = 8.6$ Hz, 2H, 2′-, 6′-H), 7.29–7.39 (*m*, 3H, 3′-, 5′-H, CH_2-***N*H**), 7.52 (d, $J = 8.4$ Hz, 1H, 8-H), 7.70 (dd, $J = 8.4$ Hz, 1.5 Hz, 1H, 7-H), 7.98 (d, $J = 5.8$ Hz, 1H, 2-H), 8.96 (d, $J = 1.5$ Hz, 1H, 5-H), 12.02 (*s*, 1H, 9-H); MS (ESI), *m/z* = 329 [M + H$^+$]; IR (ATR): 3412, 2998, 2931, 2903, 2831, 2219, 1599, 1573, 1510, 1478, 1443, 1419, 1248, 1036, 786, 767 cm^{-1}. Anal. ($C_{20}H_{16}N_4O$) Calc. C 73.2, H 4.9, N 17.1; Found C 73.0, H 4.9, N 17.5.

4–(4-Methylbenzyl)amino-9H-pyrido[2,3-b]indole-6-carbonitrile ***6c***. Yield 0.065 g (77%); brownish solid; mp 314–317 °C; ^{1}H NMR (DMSO-d_6) δ 2.24 (s, 3H, CH_3), 4.58 (d, $J = 6.5$ Hz, 2H, CH_2), 6.31 (d, $J = 5.8$ Hz, 1H, 3-H), 7.11 (d, $J = 8.0$ Hz, 2H, 3′-, 5′-H), 7.29 (d, $J = 8.0$ Hz, 2H, 2′-, 6′-H), 7.36 (*t*, $J = 6.5$ Hz, 1H, CH_2-***N*H**), 7.52 (d, $J = 8.4$ Hz, 1H, 8-H), 7.70 (d, $J = 8.4$ Hz, 1H, 7-H), 7.97 (d, $J = 5.7$ Hz, 1H, 2-H), 8.96 (d, $J = 1.5$ Hz, 1H, 5-H), 12.02 (*s*, 1H, 9-H); MS (ESI), *m/z* = 313 [M + H$^+$]; IR (ATR): 3448, 3121, 2950, 2830, 1593, 1568, 1512, 1491, 1465, 1445, 1430, 869, 786, 772 cm^{-1}. Anal. ($C_{20}H_{16}N_4$) Calc. C 76.9, H 5.2, N 17.9; Found C 77.2, H 5.5, N 17.5.

Formation of the 6-carboxy substituted 9-H-pyrido[2,3-b]indole 7

About 0.1 g (0.3 mmol) of the 6-cyano substituted benzylamine **6a** was dissolved in 5 mL of a water/diethylene glycole mixture (1:1) and 0.365 mg of sodium hydroxide and 1 mg (5.25 µmol) copper(I) iodide were added. The mixture was heated for 22 h at 150 °C under reflux. Then, the pH value was adjusted to 1 using hydrochloric acid (37%) under stirring for 1 h. Then, the precipitate was washed with diluted hydrochloric acid (0.1 M) and filtered off from the solution. Yield 0.028 g (26%); beige crystals; mp >365 °C; ^{1}H NMR (DMSO-d_6) δ 3.70 (*s*, 3H, CH_3), 4.71 (d, $J = 6.2$ Hz, 2H, CH_2), 6.50 (d, $J = 6.5$ Hz, 1H, 3-H), 6.80 (d, $J = 7.8$ Hz, 1H, 6′-H), 6.98 (d, $J = 7.8$ Hz, 1H, 4′-H), 6.99 (*s*, 1H, 2′-H), 7.24 (*t*, $J = 7.8$ Hz, 1H, 5′-H), 7.59 (d, $J = 8.5$ Hz, 1H, 8-H), 8.02 (d, $J = 6.5$ Hz, 1H, 2-H), 8.03 (dd, $J = 8.5$ Hz, 1.7 Hz, 1H, 7-H), 8.14 (br *s*, 1H, CH_2-***N*H**), 9.11 (d, $J = 1.7$ Hz, 1H, 5-H), 12.50 (*s*, 1H, 9-H), 12.71 (br *s*, 1H, COOH); MS (ESI), *m/z* = 348 [M + H$^+$]; IR (ATR): 3106, 3044, 2955, 2834, 1687, 1633, 1603, 1583, 1548, 1453, 1375, 1259, 1234, 1047, 888, 772, 738 cm^{-1}. Anal. ($C_{20}H_{17}N_3O_3$) Calc. C 69.2, H 4.9, N 12.1; Found C 69.2, H 5.1, N 12.5.

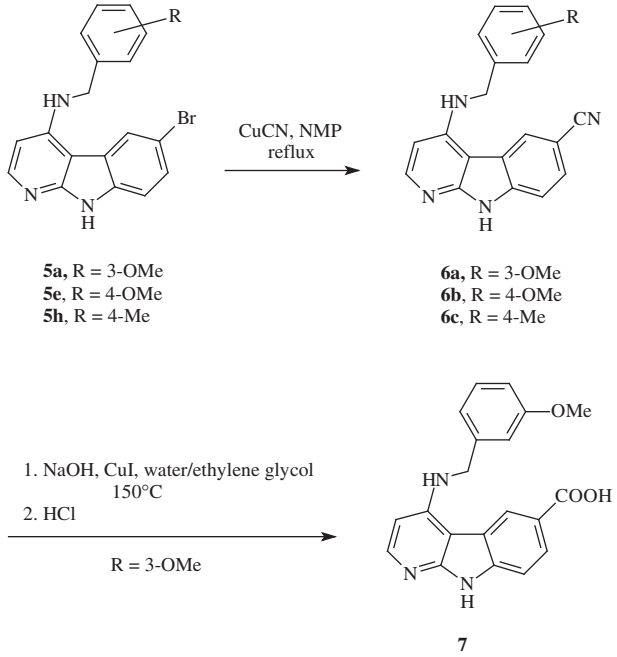

Scheme 2. Formation of 6-cyano and 6-carboxy-substituted compounds

Receptor tyrosine kinase inhibition

The protein kinases were expressed by means of the baculovirus expression system in Sf9 insect cells as human recombinant GST fusion proteins and purified by affinity chromatography using GSH-agarose. The kinase identity was confirmed by mass spectrometry using LC-ESI-MS/MS technique.

The measuring of protein kinase activity was performed in 96-well FlashPlates™ from Perkin Elmer in a 50 µL reaction volume. The reaction mixture consisted of 20 µL of assay buffer solution, 5 µL of ATP solution in water, 5 µL of used test compound in a 10% DMSO solution and finally a premixture of each 10 µL of used substrate and enzyme solutions. The assay buffer solution contained 70 mM of HEPES-NAOH pH 7.5, each 3 mM of magnesium chloride and manganese(II) chloride, 3 µM of sodium orthovanadate, 1.2 mM of DTT, 50 µg/mL of PEG_{20000} and finally 15 µM of [γ-^{33}P]-ATP making approximately 7×10^5 cpm per well.

The final kinase concentration has been 10 ng/50 µL for EGFR and IGF-1R. The used substrate was $Poly(Glu,Tyr)_{4:1}$ in a concentration of 125 ng/50 µL.

The reaction mixtures were incubated at 30 °C for 60 min. The reaction was stopped with 50 µL of a 2% (v/v) solution of

Table 1. Protein kinase inhibitory activity as determined K_i values of our target compounds **5a–h**, **6a–c** and **7** for the tyrosine receptor kinases EGFR and IGF-1R.

	K_i values [μM]	
Compound	EGFR	IGF-1R
5a	0.344 ± 0.024	9.84 ± 0.238
5z	0.361 ± 0.035	3.47 ± 0.071
5c	0.255 ± 0.018	2.96 ± 0.037
5d	0.101 ± 0.011	0.537 ± 0.022
5e	1.17 ± 0.057	2.23 ± 0.022
5f	n.a.*	2.29 ± 0.043
5g	0.448 ± 0.072	0.884 ± 0.025
5h	0.279 ± 0.091	0.697 ± 0.015
6a	0.072 ± 0.017	0.288 ± 0.026
6b	0.158 ± 0.026	0.269 ± 0.022
6c	0.160 ± 0.015	0.390 ± 0.016
7	0.140 ± 0.028	2.36 ± 0.132

*Not active.

phosphoric acid. Then, the plates were aspirated and washed twice with 200 μL of water or 0.9% solution of sodium chloride. The incorporation of ^{33}Pi was determined with a microplate scintillation counter. Ten different inhibitor concentrations were measured in a range of 3 nM to 100 μM. The residual activity (%) and the IC_{50} values were finally calculated. From the IC_{50} values, the affinity constants K_i were determined using the equation: $IC_{50} = 1/2 [E_{total}] + K_i \times (1 + [S]/K_m)$ following a competitive inhibitor binding mode[18]. The used K_m values for ATP have been measured with 1.3 μM for EGFR and with 2.52 μM for IGF-1R (Table 1).

Results and discussion

Chemistry

The benzo-anellated pyrrolo[2,3-*b*]pyridine was yielded from the primary reaction of benzotriazole and 2-bromopyridine in toluene under reflux to give the (pyridine-2-yl) benzotriazole that underwent a following polyphosphoric acid-catalyzed reaction to the tricyclic molecular scaffold. Next, a chlorination in the 4-position of the pyridine partial structure took place with phosphoryl chloride after the benzo-anellated pyrrolo[2,3-*b*]pyridine had been activated with hydrogen peroxide in acetic acid to the *N*-oxide that directed the chloro substituent preferably into the desired 4-position. Then, the bromo substituent was introduced into the preferred 6-position of the molecular scaffold using bromine in acetic acid. Finally, the varying benzylamine residues were introduced in the 4-position by heating under solvent-free conditions with the benzylamines. The bromo substituent exchange with the cyano function was managed with copper(I) cyanide by heating with NMP (*N*-methylpyrrolidone). The 6-carboxylic compound resulted from the 6-cyano substituted compound in a copper(I) iodide catalyzed reaction in strong alkaline medium.

Receptor tyrosine kinase inhibition

Insight in deregulated chemical pathways of cellular signal transduction in cancer cells offered the possibility to develop inhibitors of the responsible protein kinases[1]. Receptor tyrosine kinases are transmembrane receptor proteins that are regulated by extracellular ligands[9,18]. Being activated after ligand binding, the receptor undergoes a dimerization reaction after autophosphorylation[19,20]. The dimerized receptor activates following signal pathways by phosphorylation of respective substrates[19,21]. In the case of EGFR, which is found deregulated in many epidermal tumors, small molecule inhibitors have been developed to bind to the ATP-binding site of the receptor. Their binding is specific to single amino acid residues of the protein backbone. Mutations that cause exchanges of such amino acids led to resistance developments against established inhibitors[22]. Another recently discovered resistance mechanism of cancer cells is a possible heterodimerization of the EGFR receptor with IGF-1R as another activated tyrosine kinase[23,24]. Such described heterodimerizations made void the EGFR-specific inhibitory activity of an established EGFR inhibitor. That loss of inhibitory activity *via* receptor heterodimerization led to a proceeding of an aggressive tumor growth as described[24]. So there have been intense efforts to develop novel inhibitors of EGFR and IGF-1R.

We investigated the inhibitory activity towards both kinases EGFR and IGF-1R for our novel benzo-anellated pyrrolo[2,3-*b*]pyridines that show structural relationship to reported thienopyrimidines as EGFR inhibitors. The varied 3-benzylamine substituted compounds **5a–d** have been investigated first. The 3-methoxybenzylamine compound **5a** showed submicromolar affinities towards EGFR. The 3-chlorobenzylamine derivative **5b** showed similar EGFR affinities and the micromolar activity to inhibit IGF-1R was improved if compared to that of compound **5a**. Slight improvements of the inhibitory activity toward both kinases were found for the 3-bromobenzylamine substituted derivative **5c**. The 3-amino function in compound **5d** led to a further increased affinity toward EGFR with a K_i value of 0.101 μM and to a submicromolar affinity towards IGF-1R with 0.537 μM. So compound **5d** is a first dual inhibitor of both kinases in similar ranges. When the 3-methoxy function of compound **5a** moved to the 4-position of the benzylamine residue in derivative **5e**, the affinity towards EGFR was reduced; however, the affinity towards IGF-1R increased. If the 3-chloro function of compound **5b** moved to the 4-position of the benzylamine residue in derivative **5f**, the affinity towards EGFR was lost, while the affinity towards IGF-1R remained in the range of the 4-methoxybenzylamine compound **5e**. Finally, the movement of the 3-bromo substituent to the 4-position in the benzylamine residue of compound **5g** reduced the EGFR affinity, but increased the affinity towards IGF-1R to give a second dual inhibitor of both kinases in the similar activity range. If the 4-bromo function was replaced with a 4-methyl function in the 4-methyl benzylamino derivative **5h** both affinities increased. So we can state that a methyl function in the 4-position of the benzylamino residue is most favorable for both EGFR and IGF-1R affinities, whereas the 3-amino function is most favorable in the 3-benzylamine residue to inhibit both EGFR and IGF-1R.

We then investigated the affinity of our synthesized 5-cyano derivatives **6a–c** towards our target kinases. The 3-methoxybenzylamine compound **6a** showed significantly increased affinities towards EGFR with a determined K_i value of 72 nM. Thus, nanomolar ranges were reached similar to the EGFR inhibitor erlotinib for which a K_i value of 17.5 nM has been reported[25]. Moreover, the affinity towards IGF-1R in the submicromolar range was more than thirtyfold higher than that of the corresponding 6-bromo compound **5a**. Erlotinib for comparison showed no activity toward IGF-1R[26]. The 4-methoxybenzylamine function of compound **6b** was less favorable than the 3-methoxybenzylamine function of derivative **6a** concerning the EGFR affinity, whereas the IGF-1R affinity slightly improved. If compared to the 6-bromo compounds **5a** and **5e,** we found similar tendencies in the affinities towards EGFR and IGF-1R with the methoxy substituent in the 3-position of the benzylamine residue being more favorable towards IGF-1R, but less favorable towards EGFR. However, the 6-cyano substitution was again more favorable if compared to the 6-bromo substitution of the molecular scaffold. Finally, we determined the affinities of the 4-methyl benzylamino derivative **6c**. Both affinities towards EGFR and IGF-1R were found increased if compared to

the 6-bromo substituted compound **5h**. So we can state an allover better activity for the 6-cyano substituted compounds if compared to the 6-bromo substituted derivatives. We finally determined the affinity of the 6-carboxylic acid substituted compound **7**. The affinity towards EGFR was less favorable than that of the corresponding derivative **6a**. However, with a determined K_i value of 2.36 μM, the affinity towards IGF-1R was almost tenfold lower than that of the corresponding 6-cyano compound **6a**.

It can be summarized that we identified novel dual inhibitors of the receptor tyrosine kinases EGFR and IGF-1R. Both the benzylamine and the molecular scaffold substitutions were sensitive to influence the kinase affinities. Most favorable substitutions were the 6-cyano function of the molecular scaffold and the 3-amino and the 4-methly benzylamino residues as far as investigated. Our novel dual inhibitors may be promising lead structures to combat cancer resistance developments *via* receptor heterodimerization of the respective kinases by inhibiting both relevant kinases.

Acknowledgements

The authors acknowledge the financial support of their work by the German Research Foundation (DFG) within the project HI687/10–1 to Cornelius Hempel und Andreas Hilgeroth.

Disclosure statement

The authors report no conflicts of interest. The authors alone are responsible for the content and writing of this article.

Funding

Deutsche Forschungsgemeinschaft, 10.13039/501100001659 [HI687/10-1].

References

1. Zhang J, Yang PL, Gray NS. Targeting cancer with small molecule kinase inhibitors. Nat Rev Cancer 2009;9:28.
2. Krug M, Hilgeroth A. Recent advances in the development of multi-kinase inhibitors. Mini Rev Med Chem 2008;8:1312.
3. Li S, Schmitz KR, Jeffrey PD, et al. Structural basis for inhibition of the epidermal growth factor receptor by cetuximab. Cancer Cell 2005;7:301.
4. Yang XD, Jia XC, Corvalan JRF, et al. Eradication of established tumors by a fully human monocolonal antibody to the epidermal growth factor receptor without concomitant chemotherapy. Cancer Res 1999;59:1236.
5. Pfister DG. The just price of cancer drugs and the growing cost of cancer care: Oncologists need to be part of the solution. J Clin Oncol 2013;31:3487.
6. Lange A, Prenzler A, Frank M, et al. A systematic review of cost-effectiveness of monoclonal antibodies for metastatic colorectal cancer. Eur J Cancer 2014;50:40.
7. Scott AM, Wolchok JD, Old LJ. Antibody therapy of cancer. Nat Rev Cancer 2012;12:278.
8. Needergard MK, Hedegaard CJ, Poulsen HS. Targeting the epidermal growth factor receptor in solid tumor malignancies. BioDrugs 2012;26:83.
9. Patel R, Leung HY. Targeting the EGFR-family for therapy: biological challenges and clinical perspectives. Curr Pharm Des 2012;18:2672.
10. Warnault P, Yasri A, Coisy-Quivy M, et al. Recent advances in drug design of epidermal growth factor receptor inhibitors. Curr Med Chem 2013;20:2043.
11. Sasaki T, Hiroki K, Yamashita Y. The role of epidermal growth factor receptor in cancer metastasis and microenvironment. BioMed Res Int 2013;2013:546318. doi: http://dx.doi.org/10.1155/2013/54613.
12. Normanno N, de Luca A, Biango C, et al. Epidermal growth factor receptor (EGFR) signaling in cancer. Gene 2006;366:2.
13. Yun CH, Boggon TJ, Li Y, et al. Structure of lung-cancer derived EGFR mutants and inhibitor complexes: mechanism of activation and insights into differential inhibitor sensitivity. Cancer Cell 2007;11:217.
14. Bugge S, Kaspersen SJ, Larsen S, et al. Structure-activity study leading to identification of a highly active thienopyrimidine based EGFR inhibitor. Eur J Med Chem 2014;75:354.
15. Andrews AF, Smith DM. Synthetic approaches to some aza-analogous of benzimidazole N-oxides. Part 1. The imidazo[4,5-b]pyridine series. J Chem Soc Perkin Trans I 1982;1:2995.
16. Thutewohl M, Schirok H, Bennabi S, Figueroa-Pérez S. Synthesis of 4-substituted 7-azaindole derivatives via Pd-catalyzed C-N and C-O coupling. Synthesis. 2006;4:629.
17. Witkop B. Studies on carboline anhydronium bases. J Am Chem Soc 1953;75:3361.
18. Voigt B, Krug M, Schächtele C, et al. Probing novel 1-aza-9-oxafluorenes as selective GSK-3beta inhibitors. ChemMedChem 2008;3:120.
19. Hubbard SR, Miller WT. Receptor tyrosine kinases: mechanisms of activation and signaling. Curr Opin Cell Biol 2007;19:117.
20. Schlessinger J. Cell signalling by receptor tyrosine kinases. Cell 2000;103:211.
21. Pawson T, Gish GD, Nash P. SH2 domains, interaction modules and cellular wiring. Trends Cell Biol 2001;11:504.
22. Siegelin MD, Borczuk AC. Epidermal growth factor receptor mutations in lung adenocarcinoma. Lab Invest 2014;94:129.
23. Wang DD, Ma L, Wong MP, et al. Contribution of EGFR and ErbB-3 heterodimerization to the EGFR mutation-induced gefitinib- and erlotinib-resistance in non-small-cell lung carcinoma treatments. PLoS One 2015;10:e0128360.
24. Morgillo F, Woo JJ, Kim ES, et al. Heterodimerization of insulin-like growth factor receptor/epidermal growth factor receptor and induction of survivin expression counteract the antitumor action of erlotinib. Cancer Res 2006;66:10100.
25. Liu Y, Purvis J, Shih A, et al. A multiscale computational approach to disect early events in the Erb family receptor mediated activation, differential signaling and relevance in oncogenic transformations. Ann Biomed Engin 2007;35:1012.
26. Tandon R, Senthil V, Nithya D, et al. RBx10080307, a dual EGFR/IGF-1R inhibitor for anticancer therapy. Eur J Pharmacol 2013;711:19.